A reactive control strategy for networked hydrographical system management

Eric Duviella, Pascale Chiron, Philippe Charbonnaud

A reactive control strategy for networked hydrographical system management

Eric Duviella [a,b,*], Pascale Chiron [c], Philippe Charbonnaud [c]

[a] Univ Lille Nord de France, F-59000 Lille, France
[b] EMDouai, IA, F-59500 Douai, France
[c] Laboratoire Génie de Production, Ecole Nationale d'Ingénieurs de Tarbes, BP 1629, 65016 Tarbes Cedex, France

A B S T R A C T

A reactive control strategy is proposed to improve the water asset management of complex hydrographical systems. This strategy requires the definition of rules to achieve a generic resource allocation and setpoint assignment. A modelling method of the complex hydrographical network based on a weighted digraph of instrumented points is also presented. The simulation results of the strategy applied to a hydrographical system composed of one confluent and two diffluents show its efficiency and its effectiveness.

Keywords:
Supervision
Hybrid control accommodation
Resource allocation
Setpoint assignment
Networked systems
Water management

1. Introduction

Hydrographical systems are geographically distributed networks characterized by great dimensions and composed of dams and interconnected rivers and channels. They are used to route water volumes and satisfy Human usages. Due to the preciosity and scarcity of the water resource, the asset management of hydrographical systems became crucial. Thus, various control algorithms were proposed these last years in the literature (Malaterre & Baume, 1998; Zhuan & Xia, 2007). These methods aim at guaranteeing the setpoints and reject the disturbances in order to reduce the water losses. They were generally applied on local applications with a short-time management period. Mareels et al. (2005) underline that the quality of the irrigation service from a farmer's perspective is determined by the timing of the irrigation water. They remark also that the supervisory control has to ensure that the physical flow capacities are not exceeded. But for hydrographical systems, another risk has to be avoided: the lack of water in certain point of the network. A reactive control loop has also to guarantee ecological flows as ruled by the European Community. In Cantoni et al. (2007), an application to an open-channel irrigation network based on a distributed control structure is detailed. The network aims at supplying with water several farms. The resource consists of one reservoir. Cooperative control of water volumes using a consensus-based decision algorithm was tested with simplistic assumptions and simplifications to manage water distribution into a parallel ponds network (Tricaud & Chen, 2007). But complex hydrographical systems were not addressed. The hydrographical systems considered herein may integrate several reservoirs and rivers that introduce uncertainties. In addition, advanced methods were proposed to improve the water asset management by considering more important management period. The approach proposed in Faye, Sawadogo, Niang, and Mora-Camino (2010) allows the determination of water management objectives by the resolution of an optimization problem starting from the supervision of the network variables. It consists in adjusting the criteria and the constraints of the optimization problem. However, the complexity of the hydrographical networks and the number of the equipment to be taken into account in the optimization problem require the use of decomposition and coordination techniques of the studied systems as proposed in Mansour, Georges, and Bornard (1998). The control accommodation strategy which was proposed in Duviella, Chiron, Charbonnaud, and Hurand (2007) for one stream channels leads to the allocation of water quantities in excess toward the catchments area and of water quantities in lack amongst the users, taking into account the various requests of the users, the manager objectives, and the system constraints. This strategy is implemented since 2005 to the one stream Neste channel in the southwestern region of France and has improved the water asset management of the Neste hydrographical network. The Neste channel allows the water supply of several Gascogne rivers. The extension of this strategy to more complex

* Corresponding author at: EMDouai, IA, F-59500 Douai, France.
E-mail addresses: eric.duviella@mines-douai.fr (E. Duviella), pascale.chiron@enit.fr (P. Chiron), philippe.charbonnaud@enit.fr (P. Charbonnaud).

hydrographical systems requires new modelling solutions, and the proposal for new methods of resource allocation and setpoint assignment.

Naidu, Bhallamudi, and Narasimhan (1997) proposed a hydrographical network modelling. Indexed nodes represent the diffluences, and directed arcs the streams which connect two nodes. The exponent associated to these arcs correspond to the number of the node downstream. This representation was extended to the cases of the confluences in Islam, Raghuwanshi, Singh, and Sen (2005). The control and measurement instrumentations are taken into account by an object-oriented modelling techniques (Chan, Kritpiphat, & Tontiwachwuthikul, 1999) or an XML approach (Lisounkin, Sabov, & Schreck, 2004). It gives the representation of the elements of the hydrographical networks. In Cembrano, Wells, Quevedo, Perez, and Argelaguet (2000), modelling approaches were proposed for the optimal water management of the drinking water distribution networks and sewerage networks. For these last approaches, the representation of the control and measurement instrumentations is allowed without being adapted to integrate computation rules of the discharge propagation upstream to downstream. Finally, a modelling method of the hydrographical networks based on weighted digraph of instrumented points was proposed in Duviella, Chiron, and Charbonnaud (2007a). It was used to define and carry out a control strategy for the asset management of a hydrographical system composed of one confluence and one diffluence.

The contribution of this paper is to address the water asset management of hydrographical networks problem via generic resource allocation and setpoint assignment rules. The considered hydrographical systems are composed of several diffluences and confluences and equipped with control and measurement instrumentations. The first step of the method consists in modelling the hydrographical system and determining the transfer time delay between each equipment of the network. The second step aims at describing the reactive control strategy and proposing the resource allocation and setpoint assignment rules. The modelling method of complex hydrographical systems is presented in Section 2. In Section 3, the reactive control strategy based on resource allocation and setpoint assignment rules is proposed. Finally, the effectiveness of the strategy is shown by simulation within the framework of a hydrographical system integrating a principal stream which supplies a secondary stream for industrial and irrigation uses.

2. Complex hydrographical system modelling

Hydrographical networks consist of a finished number of *simple* hydraulic systems (HYS), *i.e.* composed of one stream. A HYS *source* is defined as a HYS which is not supplied by others HYS. A representation is proposed to locate the instrumentation, *i.e.* the sensors and the actuators, and to be able to determine the way to distribute a water quantity measured in a place of the hydrographical network, onto the whole HYS downstream. HYS are indexed by an index b, and the whole of these indices forms the set $\mathcal{B} \subset \mathbb{N}$. Each HYS is equipped with several sensors M_i^b and actuators G_j^b, with $i \in [1,m]$ and $j \in [1,n]$, where m and n are respectively the total number of measurement points and actuators which equipped the hydrographical network. Exponents will be omitted when not necessary for computation and comprehension.

It is possible to represent the structure of a hydrographical network by distinguishing two elementary configurations such as a confluence (*see* Fig. 1a), or a diffluence (*see* Fig. 1b). According to the hydraulic conditions and the conservation equations of the energy and mass, the sum of the discharges entering a node (confluence or difluence) is equal to the sum of the discharges outgoing from this node. Thus, around an operating point, the discharge q^b of the HYS b resulting from the confluence between several HYS is equal to the sum of the upstream HYS discharges, $q^b = \sum_{r \in \mathcal{C}^b} q^r$, where $\mathcal{C}^b \subset \mathcal{B}$ is the set of the HYS indices upstream to the HYS b. In addition, the HYS r resulting from the diffluence of the HYS b upstream is supplied with a proportion w_r such that the discharge q^r verifies the relation: $q^r = w_r q^b$. In order to represent diffluences, each HYS of hydrographical systems is associated to a discharge proportion w_r. For the HYS *source* and for the HYS downstream from a confluence (*see* Fig. 1a) it is equal to 1. The discharge proportion w_r of the HYS downstream the HYS b is known and such as $\forall r \in \mathcal{D}^b$, $w_r \leq 1$, and $\sum_{r \in \mathcal{D}^b} w_r = 1$, where $\mathcal{D}^b \subset \mathcal{B}$ is the set of HYS indices resulting from the diffluence of the HYS b (*see* Fig. 1b).

In the proposed modelling, the hydrographical systems are represented by a weighted digraph of instrumented points in order to determine the discharge proportions between two places of the networks. A discharge measured in a place of the hydrographical network supplies the HYS downstream of this place with discharge proportions according to the structure of the

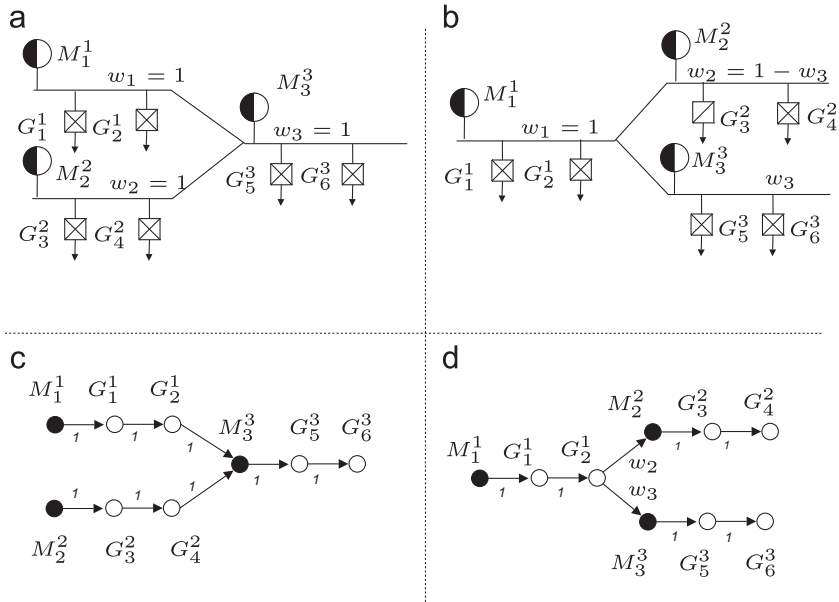

Fig. 1. (a) A confluence, (b) a diffluence, (c) its associated weighted digraph, (d) its associated weighted digraph.

hydrographical network. Thereafter, transfer time delay is introduced to evaluate the water travel time between a measurement point and the gate according to the selected path. Mareels et al. (2005) have discussed the physical meaning of the basic parameters in the grey box model (the dominant time constant, the wave period and time delay) that is presented for open-channel modelling. They derive a rule of thumb linking physical parameters like pool length, critical velocity, Manning coefficient to a reasonable first guess for the coefficients in the grey box model. Herein, an estimation technique of transfer time delay based on a physical model is described.

*Step*1: *A weighted digraph of instrumented points* is represented by a digraph composed of a succession of two types of nodes M_i or G_j (*see* Fig. 1a and d) represented respectively by full circle and circle, and arcs indicating the links between the successive nodes (*see* Fig. 1c and d). The arcs are oriented in the direction of the flow and are weighted by the discharge proportion w_r between the two nodes. The arcs from a diffluence (*see* Fig. 1d) are weighted by the discharge proportion of the HYS downstream, others are weighted by 1.

Thereafter, in order to compute all the discharge proportions from each measurement point to the gates and from every gate to the gates of the hydrographical network, an algorithm is proposed. It leads to the generation of the proportion matrix **R** composed of n lines (actuators) and $m+n$ columns (measurement points and actuators). The weighted digraph is browsed for each measurement point M_i following the algorithm given in Table 1 in order to build the proportion matrix **R**. The proposed algorithm is a classical depth-first search algorithm as proposed in Cormen, Leiserson, Rivest, and Stein (2001). This matrix contains all the discharge proportions from each measurement point to each gate, and from each gate to other gates in the hydrographical network.

*Step*2: *The value of the transfer time delays* $\mathbf{T}_{M_i,j}$ between the measurement point M_i^b and the gate G_j^d depends on the borrowed path to go from the measurement point M_i^b to the gate G_j^d (*see* Fig. 2). A direct path from M_i to G_j is a path where not other measurement point can be met between M_i and G_j. $\mathcal{P}^{b,d}$ is the set of direct paths to go from the HYS b to the HYS d, and $P_v^{b,d}$ is one of the direct paths to go from the HYS b to the HYS d, such as $P_v^{b,d} \in \mathcal{P}^{b,d}$, with $1 \le v \le \rho_{b,d}$, where $\rho_{b,d}$ denotes the total number of paths which compose $\mathcal{P}_{b,d}$.

The transfer time delays between the measurement point M_i^b and the gate G_j^d are computed by considering each path and are

Table 1
Assignment function of **R** matrix.

```
Input: weighted digraph, measurement point number m.
Output: proportion matrix R.
Initialization of R to 0
For each node N_h
  Run (N_h,N_h,1,R)
EndFor

Run (N_h,N_c,p,R),
  For each successor N_d of N_c
    p_d ← p.w_d,
    Run (N_h,N_d,p_d,R),
    If N_h is a measurement point
      If N_d is a gate
        R(d,h) ← R(d,h)+p_d
      EndIf
    Else
      If N_d is a gate
        R(d,m+h) ← R(d,m+h)+p_d
      EndIf
    EndIf
  EndFor
```

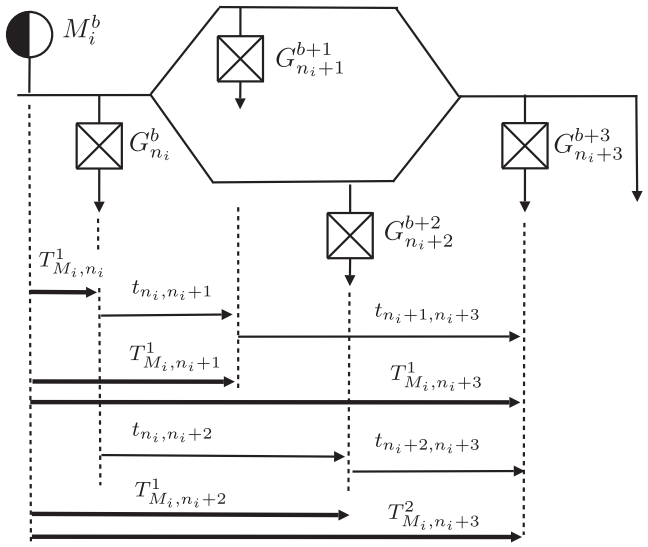

Fig. 2. Example of decomposition of transfer delays between the measurement point M_i and gates G_j.

the components of the vector $\mathbf{T}_{M_i,j}(\rho_{b,d} \times 1)$ expressed as

$$\mathbf{T}_{M_i,j} = [T_{M_i,j}^1, T_{M_i,j}^2, \ldots, T_{M_i,j}^{\rho_{b,d}}]^T, \tag{1}$$

where each component $T_{M_i,j}^v$ is an integer multiple of the sampling period T_s and computed according to

$$\begin{cases} T_{M_i,j}^v = \left\lfloor \dfrac{1}{T_s}\left(T_{M_i,n_i}^1 + \displaystyle\sum_{r=n_i}^{r=j^-} t_{r,r^+}\right)\right\rfloor + 1, \\ n_i \le j \le n, \end{cases} \tag{2}$$

where $\lfloor x \rfloor$ denotes the integer part of x, n_i is the index of the first gate downstream M_i, v is the index of the path $P_v^{b,d}$, T_{M_i,n_i}^1 is the transfer time delay between the measurement point M_i and the gate G_{n_i}, t_{r,r^+} is the transfer time delay between the gate G_r and its successor G_{r^+} along the path $P_v^{b,d}$ as illustrated in Fig. 2, and j^- is the index of the gate preceding G_j along the path $P_v^{b,d}$.

At the current time kT_s, the measured water quantity in M_i^b will reach at the gate G_j^d by the path $P_v^{b,d}$ at the time:

$$\mathcal{T}_{M_i,j}^v = (k + T_{M_i,j}^v)T_s. \tag{3}$$

The transfer delays T_{M_1,n_i}^v and $t_{r,r+}$ associated to each open-channel reach section (OCRS) are computed from the OCRS dynamics model described thereafter. An OCRS is a part of HYS defined between a measurement point and a gate, between a gate and a measurement point, or between two gates.

Usually, Saint Venant equations are used for the modelling of open-channel dynamics. The analytic resolution of these two coupled partial differential equations (Chow, Maidment, & Mays, 1988) is not possible. As discussed in Kutija and Hewett (2002) and Abbott and Basco (1989) discretization methods can be used to find a solution. Otherwise, a modelling method detailed in Litrico and Georges (1999) based on the simplification and linearization of Saint Venant equations can be used. This method is based on the identification, for each OCRS, of a transfer function plus transfer delay (4) for a reference discharge Q_e (Duviella, Chiron, & Charbonnaud, 2006), according to the OCRS geometrical characteristics:

$$F(s) = \frac{e^{-\tau s}}{1 + a_1 s + a_2 s^2}, \tag{4}$$

where the coefficients a_1, a_2 and the pure delay τ are computed according to the identified celerity and diffusion parameters C_e

Table 2
Continuous transfer functions $F(s)$ corresponding to C_L.

C_L	$F(s)$
$C_L \le \frac{4}{9}$	$\frac{1}{1+a_1 s}$
$\frac{4}{9} < C_L \le 1$	$\frac{e^{-\tau s}}{1+a_1 s}$
$1 < C_L$	$\frac{e^{-\tau s}}{1+a_1 s+a_2 s^2}$

and D_e, and to the adimensional coefficient C_L which is defined by

$$C_L = \frac{2C_e X}{9D_e}, \tag{5}$$

where X is the OCRS length, C_e and D_e are expressed as

$$\begin{cases} C_e = \dfrac{1}{L^2}\dfrac{\partial J}{\partial Q_e}\left[\dfrac{\partial L}{\partial x} - \dfrac{\partial}{\partial y}JL\right], \\ D_e = \dfrac{1}{L\dfrac{\partial J}{\partial Q_e}}, \end{cases} \tag{6}$$

where L is the surface width, y the discharge depth, J the friction slope expressed with the Manning–Strickler relation as $J = Q_e^2 P^{4/3}/K^2 S^{10/3}$, where K is the Strickler coefficient, P the wetted perimeter and S the wetted surface.

As displayed in Table 2, the order of the transfer function depends on the C_L value. When $C_L \le \frac{4}{9}$, the OCRS is short and can be modelled by a first order transfer function without delay, when $\frac{4}{9} < C_L \le 1$, a delay is added to a first order transfer function and when $C_L > 1$, the OCRS is long enough and can be modelled by a second order transfer function with delay.

The delays $T^1_{M_i,n_i}$ and t_{r,r^+} are computed from the step response of the transfer function which is identified around the reference discharge Q_e, and corresponds to the time to reach 50% of the step response. Thus, the transfer delay $T^v_{M_i,j}$ is determined (*see* Eq. (2)).

The complex hydrographical network representation, as well as the identification of the transfer time delays, constitutes an essential step for the design of reactive control strategies.

3. Resource allocation and setpoint assignment

For hydrographical networks equipped with dams located upstream and downstream on the catchment area, several management levels are usually considered. The first consists of the implementation of new dams, channels, equipments, etc., with a management horizon over 10 years. The second is the volume management level which aims at allocate the water resource amongst the catchment areas in order to supply users and to conserve a sufficient volume in the downstream dams for local supplying. The efficiency of the volume management is important for guaranteeing the balance between the stock and the demand all over on the management horizon. To achieve these objectives, managers consider weekly objective discharge. Finally, the third is the discharge management level with a sample periods of several minutes, it consists in maintaining water levels at reference setpoints value by rejecting perturbations. In this context, a reactive strategy based on supervision and hybrid control accommodation framework, accounting for second and third levels is proposed and is depicted in Fig. 3. The hydrographical network is represented by a set of m measurement points M_i and n gates G_j locally controlled. In general, the gates are controlled according to the implementation of PI controller. In recent years, other more efficient algorithms have been proposed in the literature. In Duviella et al. (2010), two control algorithms, one based on LPV approach, the second on multimodelling approach, allow effective control of gate on large operating range. Whatever the efficiency of local control is, the reactive strategy leads to the definition of new setpoints according to the capacity of each HYS, in order to avoid flood and HYS drying.

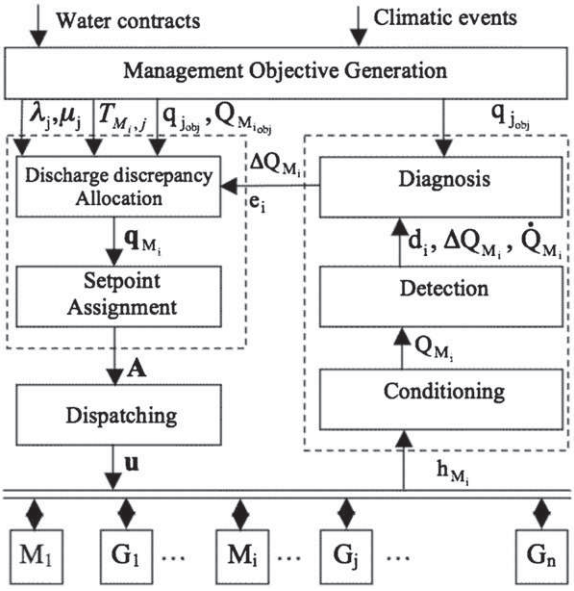

Fig. 3. Supervision and hybrid control accommodation framework for reactive control.

For each gate G_j, a weekly objective discharge $q_{j_{obj}}$ and seasonal weights λ_j and μ_j are computed by the management objective generation (MOG) module according to the water contracts and climatic events. The weights λ_j and μ_j reflect the priorities on the water uses when the resource is in excess or in lack respectively. The weekly measurement point objective discharge $Q_{M_{i_{obj}}}$ is known. The transfer time delays $\mathbf{T}_{M_i,j}$ are also given by MOG module.

For each measurement point M_i, $i = 1,\ldots,m$, discharge supervision consists in monitoring discharge disturbances and diagnosing the resource state, simultaneously. Firstly, level-meter measurements are conditioned by a low-pass filter on a sliding window which removes wrong data due to transmission errors for instance. Based on the discharge value Q_{M_i} which is determined at each time kT_s, detection and diagnosis automata are used respectively to detect a discharge discrepancy and to diagnose the resource states (Duviella et al., 2007). The sample period T_s which is chosen according to the dynamics of the hydrographical systems, generally corresponds to several minutes.

The concurrent hybrid automaton (*see* Fig. 4) is designed for each measurement point M_i. The concurrent hybrid automaton formalism is drawn from the concurrent hybrid automata proposed in Blackmore, Funiak, and Williams (2008), and Hofbaur and Williams (2002). The five pertinent states retained correspond respectively to no-discrepancy state E_0, two states where the discharge discrepancy is either positive (E^+) or negative (E^-) and constant C, and two states where the discharge discrepancy is either positive (E^+) or negative (E^-) and no constant $\neg C$. Transitions between states are defined as conditions on the measured discharge value and variation:

$$\begin{cases} d_i : [|\Delta Q_{M_i}| > th_i], \\ \psi_i : [\Delta Q_{M_i} < 0], \\ \omega_i : [|\dot{Q}_{M_i}| < dth_i], \end{cases} \tag{7}$$

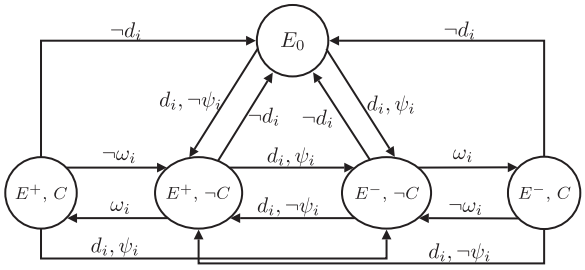

Fig. 4. Hybrid automaton for the measurement point M_i.

with

$$\Delta Q_{M_i} = Q_{M_{i_{obj}}} - Q_{M_i}, \tag{8}$$

where Q_{M_i} is the measured discharge, $Q_{M_{i_{obj}}}$ is the management objective of the measurement point M_i, $\dot{Q}_{M_i}$ the estimate derivative of Q_{M_i}, th_i and dth_i respectively the detection and diagnosis thresholds.

According to the resource state and the discharge discrepancy (*see* relation (8)), the hybrid control accommodation consists in determining the setpoints q_j, and in assigning them to the gates taking into account the hydrographical system dynamics. The resource allocation consists in recalculating setpoints with an objective to route resource excess to dams and to distribute amongst users the resource in lack. At each time kT_s, the resource allocation leads to the determination of allocation vector $\mathbf{q}_{M_i}$ which is composed of the new computed setpoints. The allocation vector is computed according to the resource state e_i taking into account the seasonal weights λ_j and μ_j.

If the resource state e_i *is* no diagnose situation (denoted E_0), the setpoints are the objective discharges $q_{j_{obj}}$. The allocation vector is such as

$$\mathbf{q}_{M_i} = [\delta^1_{\lceil R(1,i)\rceil} q_{1_{obj}} \ \ldots \ \delta^1_{\lceil R(j,i)\rceil} q_{j_{obj}} \ \ldots \ \delta^1_{\lceil R(n,i)\rceil} q_{n_{obj}}]^T, \tag{9}$$

where $\lceil \mathbf{x} \rceil$ corresponds to the higher rounding of x, n is the total number of gates, and δ^a_b the Kronecker index, is equal to 1 when $a=b$, and equal to 0 otherwise.

If the resource state e_i *is* such as discharge is in lack (denoted E^-, C) or in excess (denoted E^+, C), the water resource is allocated among the gate downstream of the measurement point M_i, according to the weights λ_j and μ_j. The allocation strategy is done by optimizing the cost function using a linear programming method for each measurement point:

$$f_{M_i} = \sum_{j=1}^{n} (\delta^1_{\lceil R(j,i)\rceil} \chi_{M_{i,j}} (q_j - q_{j_{obj}})), \tag{10}$$

with $\chi_{M_{i,j}} = \gamma 1/\lambda_j + (\gamma - 1)1/\mu_j$, $\gamma = \frac{1}{2}(\text{sign}(\Delta Q_{M_i}) + 1)$.

The optimization is carried out under four constraints:

$$\begin{cases} \sum_{j=1}^{n} (q_j - q_{j_{obj}}) = \Delta Q_{M_i}, \\ q_{j_{\min}} \le q_j \le q_{j_{\max}}, \quad 1 \le j \le n, \\ |q_j - q_{j_{obj}}| \le |R(j,i)\Delta Q_{M_i}|, \quad 1 \le j \le n, \\ q_o - q_{o_{obj}} = R(o,i)\Delta Q_{M_i} - \sum_{l=1}^{o-1} \delta^1_{\lceil R(l,i)\rceil} R(o,m+l)(q_l - q_{l_{obj}}), \quad o \in \{j | G_j \in \mathcal{O}\}, \end{cases} \tag{11}$$

where $q_{j_{\min}}$ and $q_{j_{\max}}$ are respectively the minimum and maximum discharges given for gate G_j, river or canal characteristics, δ^a_b the Kronecker index, and $\mathcal{O}$ is the set of the latest downstream controlled gates, *i.e.* the gates preceding hydrographical network outlets.

The first two constraints aim at allocating the totality of discharge discrepancies amongst the gates while preserving the new setpoints inside the operating range of each gate. The third constraint is related to the network structure. The gate G_j can absorb at the maximum $R(j,i)\Delta Q_{M_i}$ of the discrepancy measured on M_i, according to the proportion matrix $\mathbf{R}$. The fourth constraint is applied only for the latest downstream controlled gate G_o. Its objective consists in checking that the totality of discharge discrepancies is allocated on the upstream gates. In this case, the allocation vector $\mathbf{q}_{M_i}$ is such as

$$\mathbf{q}_{M_i} = [\delta^1_{\lceil R(1,i)\rceil} q_1 \ \ldots \ \delta^1_{\lceil R(j,i)\rceil} q_j \ \ldots \ \delta^1_{\lceil R(n,i)\rceil} q_n]^T. \tag{12}$$

If the resource state is such as discharge is no constant, in lack (denoted E^-,$\neg C$) or in excess (denoted E^+,$\neg C$), in order to avoid numerous re-allocation, the water resource is allocated on the smallest number of gates, taking into account the network structure. The set of selected gates have to change at each detection time, in order to avoid the control of the same gates at each time. The selection process has to allow for the weights λ_j and μ_j of gates, and the network structure. Thus, it is necessary to determine *a priori* the sets $\mathcal{L}^{\lambda}_{M_i}$ and $\mathcal{L}^{\mu}_{M_i}$ composed of sets of gates, denoted $\mathcal{L}^{\lambda}_{M_i,g}$, able to be re-allocated alternately, according to the network structure and to the proportion matrix $\mathbf{R}$. The set $\mathcal{L}^{\lambda}_{M_i}$ (resp. $\mathcal{L}^{\mu}_{M_i}$) is composed of gates which have the most important positive weights λ_j (resp. negative weights μ_j). Furthermore, each set of gates is such that the sum of the proportion coefficients given in the proportion matrix $\mathbf{R}$ for each gate of the set $\mathcal{L}^{\lambda}_{M_i,g}$ is equal to one and such that each gate of the set $\mathcal{L}^{\lambda}_{M_i,g}$ belongs to different HYS. The set $\mathcal{L}^{\lambda}_{M_i}$ of all sets $\mathcal{L}^{\lambda}_{M_i,g}$ of gates is expressed as

$$\begin{cases} \mathcal{L}^{\lambda}_{M_i,g} = \left\{ G^b_u | n_i \le u \le n, \lambda_u = \max_{1 \le j \le n} (\lambda_j) \right\}, \\ \mathcal{L}^{\lambda}_{M_i} = \left\{ \mathcal{L}^{\lambda}_{M_i,g} | \forall G^b_u, G^d_v \in \mathcal{L}^{\lambda}_{M_i,g}, u \ne v \wedge b \ne d; \sum_{u | G_u \in \mathcal{L}^{\lambda}_{M_i,g}} R(u,i) = 1 \right\}. \end{cases} \tag{13}$$

At each kT_s, because the discrepancy is not constant, the discrepancy which is not yet absorbed by the previous assigned gates Δq^k is expressed as

$$\Delta q^k = \Delta Q^k_{M_i} - \Delta Q^{k-1}_{M_i}. \tag{14}$$

The set of gates $\mathcal{L}^{\lambda}_{M_i,l}$ is selected according to the minimum and maximum discharges given for each gate G_u belonging to the set, *i.e.* $q_{u_{\min}}$ and $q_{u_{\max}}$, and to the request criterion S_l storing the number of times the set of gates $\mathcal{L}^{\lambda}_{M_i,l}$ was already requested and

Table 3
Assignment function of α and β matrices.

```
Input: weighted digraph.
Output: α_{M_i} matrix, β_{M_i} matrices
Initialization of the diagonal of α_{M_i} to 0
Initialization of β_{M_i} to 0
Run (M_i,N_{n_i},1,α_{M_i},β_{M_i})

Run (M_i,N_c,p,α_{M_i},β_{M_i})
  For any successor N_d of N_c
    p_d ← p.w_d
    If N_d is a gate
      Run (M_i,N_d,p_d,α_{M_i},β_{M_i})
      α_{M_i}(d,d) ← α_{M_i}(d,d) + p_d
      l = 1
      While (β_{M_i}(l,d) ≠ 0)
        l++
      EndWhile
      β_{M_i}(l,d) ← p_d
    EndIf
  EndFor
```

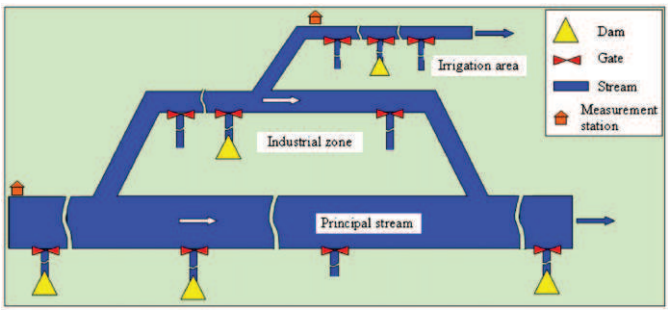

Fig. 5. Networked hydrographical system.

Table 4
Gate parameters.

Gate	$q_{j_{obj}}$	$q_{j\,\min}$	$q_{j\,\max}$	λ_j	μ_j
G_1^1	1	0.3	5	10	1
G_2^2	1	0.25	3	1	1
G_3^2	1.5	0.5	3.5	10	1
G_4^3	0.8	0.2	2	1	10
G_5^3	0.3	0.15	2.5	10	1
G_6^3	0.6	0.15	2	1	10
G_7^4	0.9	0.2	2.5	1	10
G_8^5	4	1	7	10	1
G_9^5	2	0.5	5	1	10
G_{10}^6	0.5	0.1	3	10	1
G_{11}^3	0.4	0.2	1	–	–
G_{12}^6	8	4	10	–	–

associated to each set of gates (it is a similar procedure for $\mathcal{L}^{\mu}_{M_i,l}$):

$$\begin{cases} l|S_l = \min\limits_{g|\mathcal{L}^{\lambda}_{M_i,g} \in \mathcal{L}^{\lambda}_{M_i}} S_g, \\ \forall G_u \in \mathcal{L}^{\lambda}_{M_i\,l}, \quad q_{u_{\min}} \le q_u^{k-1} + R(u,i)\Delta q^k \le q_{u_{\max}}. \end{cases} \tag{15}$$

Then, the allocation vector $\mathbf{q}^k_{M_i}$ is given by

$$\begin{cases} \mathbf{q}^k_{M_i} = [\delta^1_{R(1,i)}(q_1^{k-1} + B_1 R(i,1)\Delta q^k) \ \ldots \ \delta^1_{R(u,i)}(q_u^{k-1} + B_u R(i,u)\Delta q^k) \\ \quad \ldots \ \delta^1_{R(n,i)}(q_n^{k-1} + B_n R(i,n)\Delta q^k)]^T, \\ \text{with } B_u = \begin{cases} 1 & \text{if } G_u \in \mathcal{L}^{\lambda}_{M_i,l}, \\ = 0 & \text{otherwise.} \end{cases} \end{cases} \tag{16}$$

Then, the new setpoints must be assigned to the gates at a time taking into account the transfer delays. Two setpoint assignment rules were defined and compared in the case of networked hydrographical systems in Duviella, Chiron, and Charbonnaud (2007b). The setpoint assignment rule which leads to the best performances consists in considering the several direct transfer delays $\mathbf{T}_{M_i,j}$ (*see* relation (1)) starting from M_i to each gate G_j. Due to these paths, it is necessary to consider supplying discharge proportions $\boldsymbol{\beta}_{M_i}(v,j)$ which correspond to the discharge resulting from M_i^b and supplying G_j^d by the path $P_v^{b,d}$. The supplying discharge proportion $\boldsymbol{\beta}_{M_i}$ $(\rho_{M_i} \times n)$, where ρ_{M_i} is the maximum number of paths between M_i and all the gates G_j, is computed for each measurement point M_i according to the algorithm given in Table 3 and the weighted digraph of the system.

The set of allocation times starting from M_i is denoted $\boldsymbol{\Gamma}_{M_i}$ $(\rho_{M_i} \times n)$. The matrix $\boldsymbol{\Gamma}_{M_i}$ is updated at each sampling period

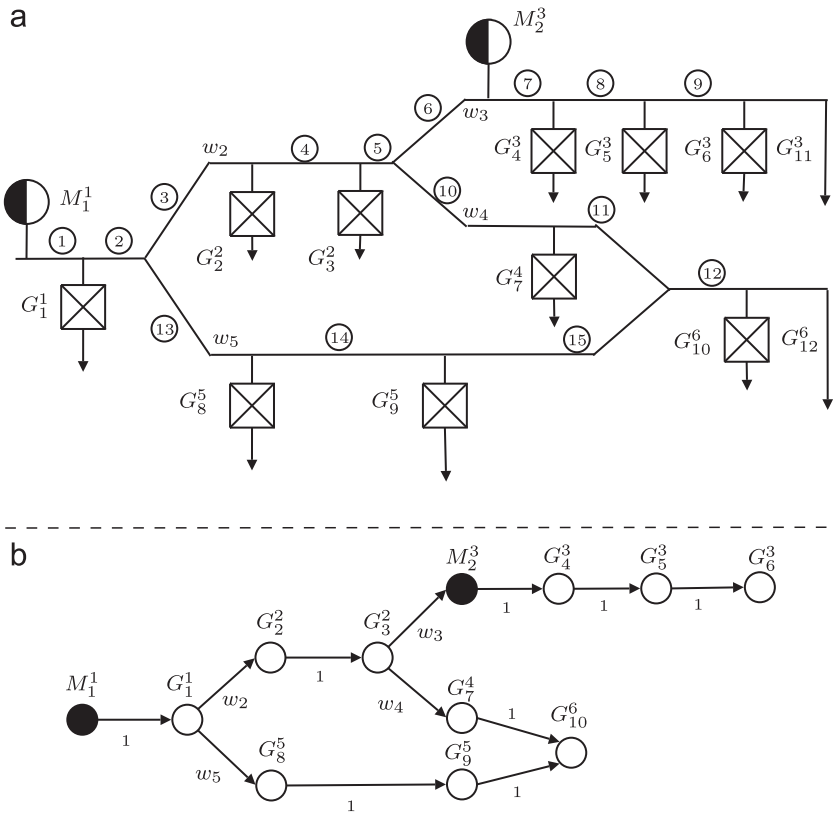

Fig. 6. (a) Networked hydrographical system representation, (b) its associated digraph representation for **R** and $\boldsymbol{\alpha}_{Mi}$ determination.

T_s and its elements are expressed by

$$\Gamma_{M_i}(v,j)=\begin{cases} T^{v}_{M_i,j} & \text{if } n_i \le j \le n \text{ and } 1 \le v \le \rho_{b,d}, \\ 0 & \text{if } (1 \le j < n_i) \text{ or } (n_i \le j \le n \text{ and } \rho_{b,d} < v \le \rho_{M_i}), \end{cases} \tag{17}$$

where $\mathcal{T}^{v}_{M_i,j}$ is defined by Eq. (2).

At each time kT_s, the setpoint assignment matrix $\mathbf{A}^{k}_{M_i}$ $(H_{M_i} \times n)$, where H_{M_i} is the allocation horizon from M_i, is scheduled according to $\mathbf{\Gamma}_{M_i}$ and $\mathbf{q}_{M_i}$. The allocation horizon H_{M_i} corresponds to the greatest transfer delay from M_i which is expressed according to T_s. The first row of $\mathbf{A}^{k}_{M_i}$ contains the setpoints to be assigned to each gate from M_i at the time $(k+1)T_s$, the hth row the ones to be assigned at the time $(k+h)T_s$ as defined in Eq. (18), and the last row the ones to be assigned at time $(k+H_{M_i})T_s$:

$$A^{k}_{M_i}(h,j)=\begin{cases} \sum_{v=1}^{\rho_{M_i}} \varphi_v \boldsymbol{\beta}_{M_i}(v,j) q_{M_i}(j) & \text{if } \exists v \text{ such as } \mathcal{T}^{v}_{M_i,j} \le (k+h)T_s, \\ A^{k-1}_{M_i}(h+1,j) & \text{else if } 1 \le h < H_{M_i}, \\ q_{j_{obj}} & \text{otherwise}, \end{cases} \tag{18}$$

where $\varphi_v = 1$ if $\Gamma_{M_i}(v,j) \ge (k+h)T_s$, $\varphi_v = 0$ otherwise, and $A^{0}_{M_i}(h,j) = q_{j_{obj}}$.

The setpoints are dispatched with the control period $T_c = \kappa T_s$, where κ is an integer. The control setpoint vector denoted $\mathbf{u}$ $(1 \times n)$ is updated at each time $k'T_c$, where $k' = k/\kappa$, thanks to the assignment matrix $\mathbf{A}^{k'}_{M_i}$ and the $\boldsymbol{\alpha}_{M_i}$ $(n \times n)$ diagonal control accommodation matrix, with $H = (1/\kappa)\max_{1 \le i \le m}(H_{M_i})$ the control horizon which corresponds to the greatest transfer delay expressed according to T_c. For each measurement point M_i, the $\boldsymbol{\alpha}_{M_i}$ matrix, the role of which is to capture the measurement point influence on the gates, must be determined. In order to generate the $\boldsymbol{\alpha}_{M_i}$ matrix, the weighted digraph (*see* Fig. 1c and d) is browsed using the algorithm given in Table 3, for each measurement point M_i.

The control setpoint vector $\mathbf{u}^{k'}$ $(1 \times n)$ is calculated by

$$u^{k'}(j) = \sum_{i=1}^{m} \boldsymbol{\alpha}_{M_i}(j,j) A^{k'}_{M_i}(1,j). \tag{19}$$

The setpoint dispatching leads to the application of the most recently calculated setpoints. This method increases the control strategy reactivity and its robustness in performance, because resource states have been diagnosed in real time and discharge variations between two control times are taken into account.

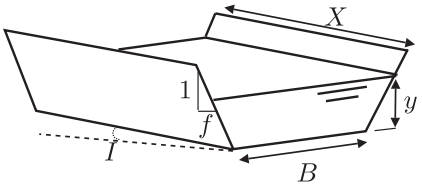

Fig. 7. Geometrical characteristics of a trapezoidal profile.

4. Simulation results

The networked hydrographical system which is considered in this article (*see* Fig. 5) consists of a principal stream which supplies a secondary stream for industrial and irrigation uses. This system is equipped with two measurement stations and 10 controlled gates. PI controller is designed for each controlled gate. A telecontrol system allows the flow discharges measurement and the gate control at distance. These controlled gates supply other streams for various uses, and catchment areas downstream to stock the volume of water.

The hydrographical system is subjected to disturbances which are naturally routed from upstream to downstream and make not possible to satisfy the uses. Disturbances are from natural disorders like strong local rain or from human activities, like industrial and agricultural activities. Thus, an efficient water asset management consists in avoiding overflow and lack of water at the ends of the network, to valorize the water in lack fairly done between users and to stock in dams the water in excess. The proposed strategy which satisfies these objectives is evaluated in this case.

The hydrographical system is composed of one confluence and two diffluences. The six HYS are equipped with 10 gates, G^{1}_{1}–G^{6}_{10}, and two measurement points M^{1}_{1} and M^{3}_{2}. The HYS 1 supplies the HYS 2 and the HYS 5 with the discharge proportions w_2 and w_5, respectively; the HYS 2 supplies the HYS 3 and the HYS 4 with the discharge proportions w_3 and w_4. Finally, the HYS 4 and 5 supply the HYS 6. The discharge proportion w_2 is equal to 0.3, w_5 to 0.7, w_3 to 0.6 and w_4 to 0.4. These proportions are constant around the considered operating point. The hydrographical outputs are noted G^{3}_{11} and G^{6}_{12}, but they are not controlled. The indices of the gates G^{6} and G^{10} which are located just upstream these canal outputs,

Table 5
Geometrical characteristics of the OCRS.

OCRS	*B* (m)	*f*	*X* (m)	*I*	*K*
1	6	0.8	1000	5×10^{-4}	70
2	6	0.8	200	5×10^{-4}	70
3	2	0.6	4000	5×10^{-4}	70
4	2	0.6	600	5×10^{-4}	70
5	2	0.6	100	5×10^{-4}	70
6	2	0.6	500	2×10^{-4}	70
7	2	0.6	3000	2×10^{-4}	70
8	2	0.6	1500	3×10^{-4}	70
9	2	0.6	2000	3×10^{-4}	70
10	0.6	0.95	3000	3×10^{-4}	70
11	0.6	0.95	1500	3×10^{-4}	70
12	6	0.8	2000	2×10^{-4}	70
13	6	0.8	5000	4×10^{-4}	70
14	6	0.8	2000	4×10^{-4}	70
15	6	0.8	3000	3×10^{-4}	70

Table 6
Continuous transfer function of the OCRS.

OCRS	Q_e	a_1	a_2	τ	*t* (s)
1	20	445	0	0	310
2	20	90	0	0	60
3	6	1810	0	755	2000
4	5	406	0	0	280
5	3	70	0	0	50
6	2	575	0	0	400
7	2	3450	0	0	2380
8	1	1590	0	75	1180
9	1	1840	0	385	1660
10	1	3020	0	820	2910
11	1	1300	0	0	900
12	8	1560	0	0	1080
13	14	1750	0	870	2090
14	10	1080	0	70	820
15	8	1760	0	250	1470

compose the set $\mathcal{O}=\{6,10\}$. The gate characteristics, *i.e.* objective discharge $q_{j_{obj}}$, maximum and minimum discharges $q_{j_{max}}$, $q_{j_{min}}$, and their associated weights, are given in Table 4. Maximum and minimum discharges are determined according to the capacity of each HYS.

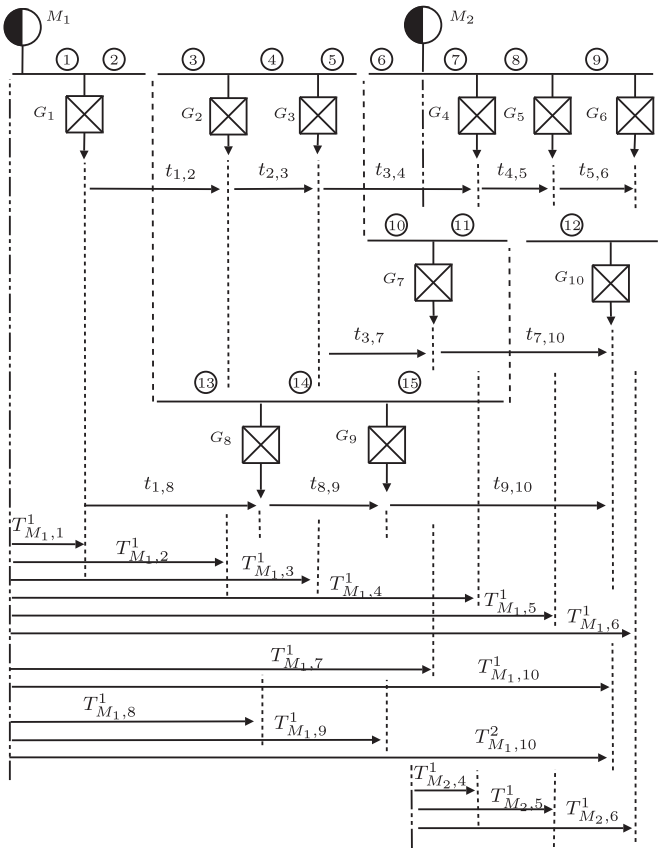

Fig. 8. Time delays between measurement points and gates.

To apply the proposed strategy, the first step consists in modelling the network. The hydrographical system (*see* Fig. 5) is represented by the weighted digraph depicted in Fig. 6 to determine the matrices $\mathbf{R}$, $\boldsymbol{\alpha}_{M_i}$ and $\boldsymbol{\beta}_{M_i}$, according to the algorithms given in Tables 1 and 3 respectively. The matrix $\mathbf{R}$ is given by relation (22). The diagonal matrices $\boldsymbol{\alpha}_{M_1}$ and $\boldsymbol{\alpha}_{M_2}$ are given by

$$\boldsymbol{\alpha}_{M_1} = diag\{1,0.3,0.3,0,0,0,0.12,0.7,0.7,0.82\},$$

$$\boldsymbol{\alpha}_{M_2} = diag\{0,0,0,1,1,1,0,0,0,0\}. \tag{20}$$

The matrices $\boldsymbol{\beta}_{M_1}$ and $\boldsymbol{\beta}_{M_2}$ are given by

$$\boldsymbol{\beta}_{M_1} = \begin{bmatrix} 1 & 0.3 & 0.3 & 0 & 0 & 0 & 0.12 & 0.7 & 0.7 & 0.12 \\ 0 & 0 & 0 & 0 & 0 & 0 & 0 & 0 & 0 & 0.7 \end{bmatrix},$$

$$\boldsymbol{\beta}_{M_2} = [0\ 0\ 0\ 1\ 1\ 1\ 0\ 0\ 0\ 0]. \tag{21}$$

The values of $\boldsymbol{\alpha}_{M_1}$, *i.e.* from the measurement point M_1 to the gates, are equal to 0 for the gates G_4–G_6 because there is no direct path between M_1 and these gates. For the other gates, the proportions w_i associated to each diffluence are taken into account.

The value of $\mathbf{R}(j,1)$, *i.e.* from the measurement point M_1 to the gates, is equal to 1 for the gate G_1 because there is no diffluence between this measurement point and this gate, and equal to 0.82 ($0.3\times0.4+0.7$) for the gate G_{10} taking into account the two paths existing from M_1 to G_{10} and the proportions w_i associated to each diffluence. The value of $\mathbf{R}(j,m+2)$, *i.e.* from the gate G_2 to the other gates ($m=2$), is equal to 0 for upstream gates like G_1, equal to 1 for gates on the same HYS like G_2 and G_3, and equal to 0.6 for

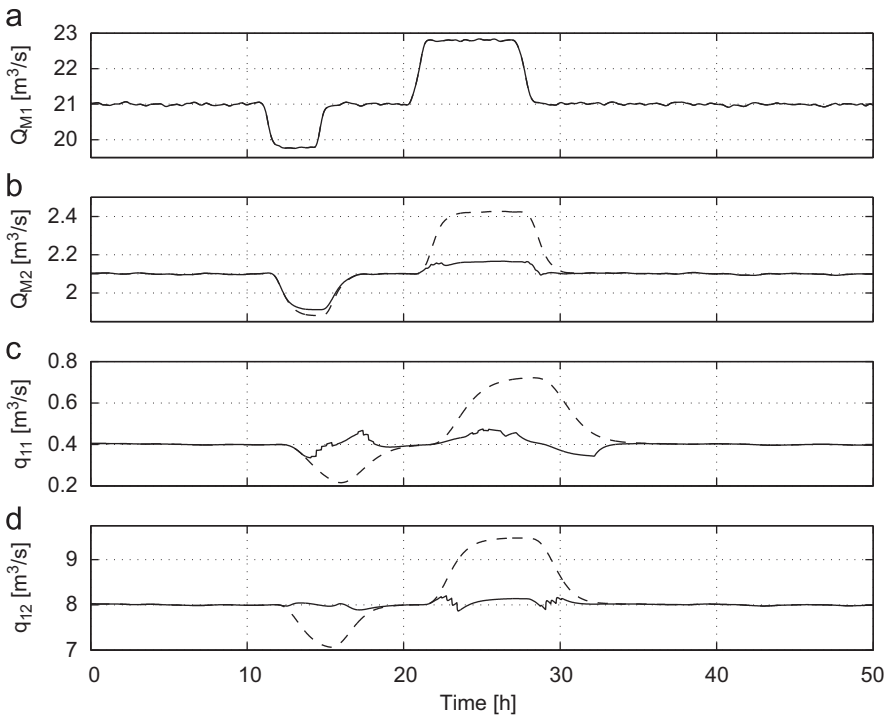

Fig. 9. Discharges with (continuous line) and without (dashed line) reactive control strategy (a) Q_{M_1}, (b) Q_{M_2}, and resulting discharges on (c) G_{11} and (d) G_{12}.

gates G_4 and G_6 because of the diffluence:

$$\mathbf{R} = \begin{bmatrix} 1 & 0 & 0 & 0 & 0 & 0 & 0 & 0 & 0 & 0 & 0 & 0 \\ 0.3 & 0 & 0.3 & 0 & 0 & 0 & 0 & 0 & 0 & 0 & 0 & 0 \\ 0.3 & 0 & 0.3 & 1 & 0 & 0 & 0 & 0 & 0 & 0 & 0 & 0 \\ 0.18 & 1 & 0.18 & 0.6 & 0.6 & 0 & 0 & 0 & 0 & 0 & 0 & 0 \\ 0.18 & 1 & 0.18 & 0.6 & 0.6 & 1 & 0 & 0 & 0 & 0 & 0 & 0 \\ 0.18 & 1 & 0.18 & 0.6 & 0.6 & 1 & 1 & 0 & 0 & 0 & 0 & 0 \\ 0.12 & 0 & 0.12 & 0.4 & 0.4 & 0 & 0 & 0 & 0 & 0 & 0 & 0 \\ 0.7 & 0 & 0.7 & 0 & 0 & 0 & 0 & 0 & 0 & 0 & 0 & 0 \\ 0.7 & 0 & 0.7 & 0 & 0 & 0 & 0 & 0 & 0 & 1 & 0 & 0 \\ 0.82 & 0 & 0.82 & 0.4 & 0.4 & 0 & 0 & 0 & 1 & 1 & 1 & 0 \end{bmatrix}. \quad (22)$$

The second step consists in modelling the HYS according to the specific length and profile section of each OCRS, to determine the transfer time delays $\mathbf{T}_{M_i,j}$. The OCRS are numbered from 1 to 15 (*see* Fig. 6a). The OCRS with trapezoidal profile is characterized by the bottom width B, the average fruit of the banks f, the profile length X, the discharge depth y and the slope I (*see* Fig. 7). The geometrical characteristics of the OCRS are given in Table 5.

For trapezoidal profiles, the celerity and diffusion parameters C_e and D_e are expressed as

$$\begin{cases} C_e = \dfrac{Q_e}{L^2}\left[-f + \dfrac{L}{3}\left(\dfrac{2B}{Py} + \dfrac{5L}{S} - \dfrac{2}{y}\right)\right], \\ D_e = \dfrac{Q_e}{2LJ}, \end{cases} \quad (23)$$

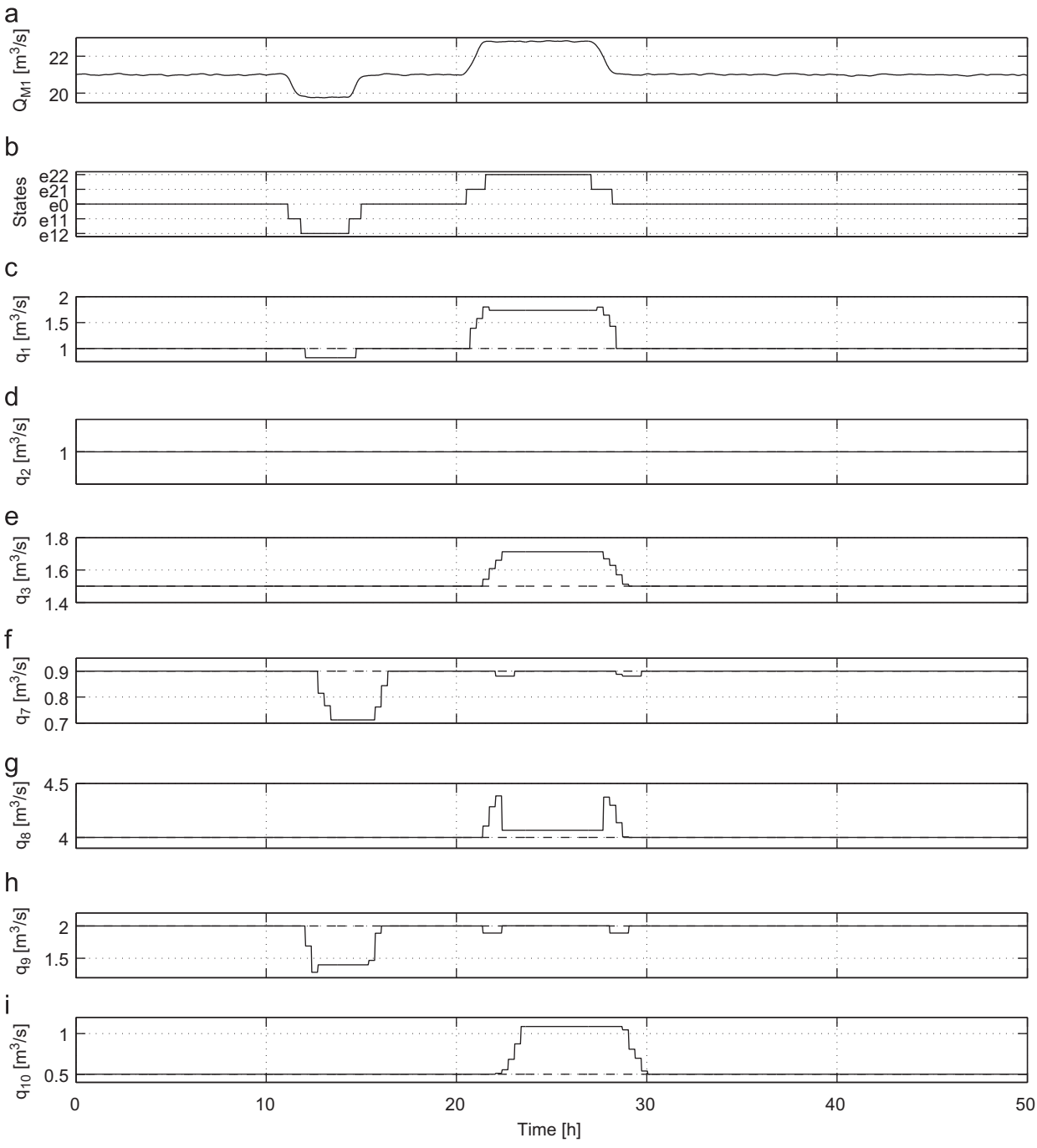

Fig. 10. (a) Discharge Q_{M_1}, (b) diagnosed states from M_1. Setpoint assigned, with (continuous line) and without (dashed line) reactive control strategy, to (c) gate G_1, (d) gate G_2, (e) gate G_3, (f) gate G_7, (g) gate G_8, (h) gate G_9 and (i) gate G_{10}.

with $L=B+2fy$, $S=yB+fy^2$, $P=B+2y\sqrt{1+f^2}$, and the slope J is equivalent to the reach slope I for a non-critical discharge.

In the studied case, the transfer function is estimated for one operating point for each OCRS. Parameters of the transfer functions identified for reference discharges, Q_e, are given in Table 6. The response time t is computed from the step response of every identified model so that 50% of the step response is reached. Then, the transfer delays $T^v_{M_i,j}$ are calculated using Eq. (2) and the sample time T_s (equal to 120 s), while computing the transfer delays $T^v_{M_i,n_i}$ and t_{r,r^+} with the response time t according to the hydrographical network configuration (*see* Fig. 8).

Finally, the transfer time delays $T^v_{M_i,j}$ are used to determine, according to relation (17), the matrices $\mathbf{\Gamma}_{M_1}$ and $\mathbf{\Gamma}_{M_2}$:

$$\mathbf{\Gamma}_{M_1}=\begin{bmatrix}3,20,23,0,0,0,47,21,28,49\\0,\ 0,\ 0,\ 0,\ 0,\ 0,\ 0,\ 0,\ 0,\ 64\end{bmatrix}^T, \tag{24}$$

$$\mathbf{\Gamma}_{M_2}=[0,0,0,20,30,44,0,0,0,0]^T. \tag{25}$$

Taking into account the network structure, the fourth constraints defined by (11) are specified for the measurement point M_1 as relation (26) and for the measurement point M_2 as relation (27):

$$\begin{cases} q_6-q_{6_{obj}}=R(6,1)\Delta Q_{M_1}-R(6,3)(q_1-q_{1_{obj}})-R(6,4)(q_2-q_{2_{obj}})\\ \quad -R(6,5)(q_3-q_{3_{obj}})-R(6,6)(q_4-q_{4_{obj}})-R(6,7)(q_5-q_{5_{obj}}),\\ q_{10}-q_{10_{obj}}=R(10,1)\Delta Q_{M_1}-R(10,3)(q_1-q_{1_{obj}})-R(10,4)(q_2-q_{2_{obj}})\\ \quad -R(10,5)(q_3-q_{3_{obj}})-R(10,9)(q_7-q_{7_{obj}})-R(10,10)(q_8-q_{8_{obj}})\\ \quad -R(10,11)(q_9-q_{9_{obj}}), \end{cases} \tag{26}$$

where the values of $R(j,1)$ are provided by the relation (22):

$$q_6-q_{6_{obj}}=R(6,2)\Delta Q_{M_2}-R(6,6)(q_4-q_{4_{obj}})-R(6,7)(q_5-q_{5_{obj}}), \tag{27}$$

where the values of $R(j,2)$ are provided by relation (22).

According to the network structure, the sets $\mathcal{L}_{M_1}$ and $\mathcal{L}_{M_2}$ of sets of gates able to be re-allocated is given by relation (28) for water in excess, and by relation (29) for water in lack.

$$\begin{cases} \mathcal{L}^{\lambda}_{M_1}=\{\{G_1\},\{G_3,G_8\},\{G_5,G_{10}\}\},\\ \mathcal{L}^{\mu}_{M_1}=\{\{G_4,G_7,G_9\},\{G_6,G_7,G_9\}\}. \end{cases} \tag{28}$$

$$\begin{cases} \mathcal{L}^{\lambda}_{M_2}=\{\{G_5\}\},\\ \mathcal{L}^{\mu}_{M_2}=\{\{G_4\},\{G_6\}\}. \end{cases} \tag{29}$$

The objective discharges of M_1 and M_2 correspond respectively to 21 and 2.1 m^3/s. The hydrographical system is subjected to disturbances upstream of the measurement points M_1 (*see* Fig. 9a). The measured discharge on M_2 is shown in Fig. 9b. The discharges resulting at the canal ends G_{11} and G_{12} in the case where no reactive strategy is used (dashed line) and where the reactive strategy is applied (continuous line) are shown in Fig. 9c and d. Figs. 10 and 11 show the measured discharges in (a), the corresponding resource states diagnosis in (b), and the new setpoints which have been dispatched at the gates in continuous line when the strategy is applied and in dashed line when it is not applied. The diagnosed resource state on M_1 is depicted in Fig. 10b, and the setpoints dispatched on gates G_1, G_2, G_3, G_7, G_8 G_9 and G_{10} respectively in Figs. 10c–i. Fig. 11b shows the diagnosed resource state on M_2, and the setpoints dispatched on gates G_4, G_5 and G_6 respectively in Figs. 11c–e.

When the reactive control strategy is used, nearly 84% of the discrepancy volumes upstream M_1 are allocated amongst the

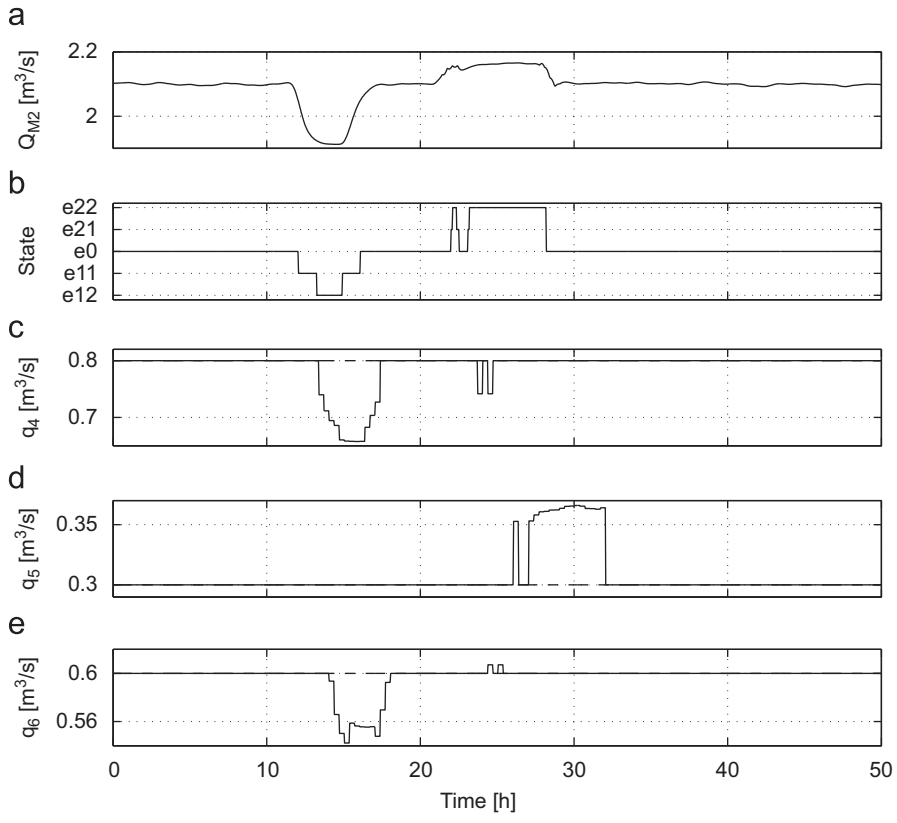

Fig. 11. (a) Discharge Q_{M_2}, (b) diagnosed states from M_2. Setpoint assigned, with (continuous line) and without (dashed line) reactive control strategy, to (c) gate G_4, (d) gate G_5 and (e) gate G_6.

gates according to their weights. This strategy leads to a water dispatching of 52 000 m^3 among the 62 000 m^3 of discrepancy volumes during 50 h. The water volumes are conserved by their storage in dams, and represent 19 500, 5000, 1200, 3000 and 13 500 m^3 for dam downstream G_1, G_3, G_5, G_8 and G_{10} respectively. Moreover, the discharges at the end of the hydrographical system are close to the objective values 0.4 m^3/s for G_{11} and 8 m^3/s for G_{12} (*see* Fig. 9c and d). The discharge discrepancies around the objective values on G_{11} and G_{12} do not exceed 0.07 and 0.2 m^3/s respectively.

5. Conclusion

The resource allocation and setpoint assignment rules have been defined to cope with the water asset management of complex hydrographical systems. It is a generic approach allowing the water resource valorization whatever the configuration of the hydrographical networks is. Multiple graph representations make it possible to identify the information for implementing the proposed supervision and hybrid control accommodation strategy. The simulation results show the effectiveness of the strategy which is efficient to manage the water resource in the case of a complex hydrographical system.

References

Abbott, M. B., & Basco, D. (1989). *Computational fluid dynamics: An introduction for engineers*.

Blackmore, L., Funiak, S., & Williams, B. C. (2008). A combined stochastic and greedy hybrid estimation capability for concurrent hybrid models with autonomous mode transitions. *Journal of Robotics and Autonomous Systems*, *56*, 105–129.

Cantoni, M., Weyer, E., Li, Y., Ooi, S., Mareels, I., & Ryan, M. (2007). Control of large-scale irrigation networks. In J. Bailliuel, P. Antsaklis (Eds.), *Proceedings of the IEEE, special issue on the technology of networked control systems* (Vol. 95, pp. 75–91).

Cembrano, G., Wells, G., Quevedo, J., Perez, R., & Argelaguet, R. (2000). Optimal control of a water distribution network in a supervisory control system. *Control Engineering Practice*, *8*, 1177–1188.

Chan, C., Kritpiphat, W., & Tontiwachwuthikul, P. (1999). Development of an intelligent control system for a municipal water distribution network. In *IEEE CCECE* (Vol. 99(2), pp. 1108–1113).

Chow, V. T., Maidment, D. R., & Mays, L. W. (1988). *Applied hydrology*.

Cormen, T. H., Leiserson, C. E., Rivest, R. L., & Stein, C. (2001). *Introduction to algorithms* (2nd ed.).

Duviella, E., Chiron, P., & Charbonnaud, P. (2006). Multimodelling steps for free-surface hydraulic systems control. In *ICINCO 06*, Setubal, Portugal, August 1–5.

Duviella, E., Chiron, P., & Charbonnaud, P. (2007a). Modelling, resource allocation and setpoints assignment of complex hydrographical system. In *LSS'07*, Gdansk, Pologne, July 23–25.

Duviella, E., Chiron, P., & Charbonnaud, P. (2007b). Setpoints assignment rules based on transfer time delays for water asset-management of networked open-channel systems. In *ICINCO 07* (pp. 312–319), Angers, France, May 9–12.

Duviella, E., Chiron, P., Charbonnaud, P., & Hurand, P. (2007). Supervision and hybrid control accommodation for water asset management. *Control Engineering Practice*, *15*, 17–27.

Duviella, E., Puig, V., Charbonnaud, P., Escobet, T., Carrillo, F., & Quevedo, J. (2010). Supervised gain-scheduling multimodel versus linear parameter varying internal model control of open-channel systems for large operating conditions. *ASCE Journal of Irrigation and Drain Engineering*, *136*, 543–552. doi:10.1061/(ASCE)IR.1943-4774.0000219.

Faye, R. M., Sawadogo, S., Niang, A., & Mora-Camino, F. (2010). An intelligent decision support system for irrigation system management. *IEEE SMC 98* (Vol. 4, pp. 3908–3913), San Diego, USA, October 11–14.

Hofbaur, M. W., & Williams, B. C. (2002). Hybrid diagnosis with unknown behavioral modes. In *International workshop on principles of diagnosis (Dx-02)* (pp. 97–105), Semmering, Austria, May 2–4.

Islam, A., Raghuwanshi, N. S., Singh, R., & Sen, D. J. (2005). Comparison of gradually varied flow computation algorithms for open-channel network. *Journal of Irrigation and Drainage Engineering*, *131*, 457–465.

Kutija, V., & Hewett, C.-J.-M. (2002). Modelling of supercritical flow conditions revisited; NewC scheme. *Journal of Hydraulic Research*, *40*, 145–152.

Lisounkin, A., Sabov, A., & Schreck, G. (2004). Interpreter based model check for distribution networks. In *IEEE INDIN O4* (pp. 431–435), June 24–26.

Litrico, X., & Georges, D. (1999). Robust continuous-time and discrete-time flow control of a dam-river system. (i) Modelling. *Applied Mathematical Modelling*, *23*, 809–827.

Malaterre, P.-O., & Baume, J.-P. (1998). Modeling and regulation of irrigation canals: Existing applications and ongoing researches. In *IEEE international conference on systems, man, and cybernetics* (Vol. 4, pp. 3850–3855).

Mansour, H. E. F., Georges, D., & Bornard, G. (1998). Optimal control of complex irrigation systems via decomposition-coordination and the use of augmented lagrangian. In *IEEE CCA 98* (pp. 3874–3879), Trieste, Italy.

Mareels, I., Weyer, E., Ooi, S., Cantoni, M., Li, Y., & Nair, G. (2005). Systems engineering for irrigation systems: Successes and challenges. *Annual Reviews in Control*, *29*, 191–204.

Naidu, B. J., Bhallamudi, S. M., & Narasimhan, S. (1997). Computation in tree-type channel networks. *Journal of Hydraulic Engineering*, *123*, 700–708.

Tricaud, C., & Chen, Y.-Q. (2007). Cooperative control of water volumes of parallel ponds attached to an open channel based on information consensus with minimum diversion water loss. In *International conference on mechatronics and automation*, *ICMA 2007* (pp. 3283–3288), Harbin, China, August 5–8.

Zhuan, X., & Xia, X. (2007). Models and control methodologies in open water flow dynamics: A survey. In *IEEE Africon* (Vol. 7, pp. 1–7).